JOC Article

Self-Assembly of Molecular Nanoball: Design, Synthesis, and Characterization

Sushobhan Ghosh and Partha Sarathi Mukherjee*

Department of Inorganic and Physical Chemistry, Indian Institute of Science, Bangalore-560012, India

psm@ipc.iisc.ernet.in

Received June 26, 2006

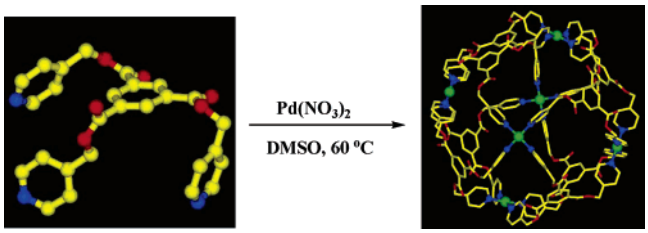

The design and self-assembly of two new flexible supramolecular nanoballs are described. These assemblies incorporate two flexible tritopic amide and ester building blocks and were prepared in excellent yields (96−97%) via coordination driven self-assembly. The first resulted from the reaction of 4 equiv of a new tritopic ester ligand *N*,*N*′,*N*″-tris(4-pyridylmethyl) trimesic ester and 3 equiv of C_4 symmetric Pd-$(NO_3)_2$. The second analogous structure was obtained by the self-assembly of a flexible *N*,*N*′,*N*″-tris(3-pyridylmethyl) trimesic amide and $Pd(NO_3)_2$. The assemblies were characterized with multinuclear NMR spectroscopy, electrospray ionization mass spectroscopy, elemental analysis, and TGA. Mass spectrometry along with NMR data and TEM view confirms the existence of the two assemblies. MM2 force field simulations of the cages showed a ball shape with the diameter of the inner cavity of about 2.1 and 1.8 nm for **2a** and **2b**, respectively, which were also corroborated by TEM analysis.

Introduction

Stepwise covalent synthesis of large molecules is often time-consuming and laborious and thus generally ends in a low yield of the target product. It is also difficult to achieve a large desired product where the controlling force is a nondirectional weak interaction like hydrogen bonding, van der Waals, and $\pi-\pi$ interaction. Instead, by utilizing the stronger metal−ligand directional coordination bonding approach, one can easily prepare the desired large molecules using appropriate molecular units.[1] The major requirement for this coordination-driven self-assembly approach is the use of rigid precursors of appropriate size and shapes. Square-planar Pt(II) and Pd(II) have long been used as favorite metals in this area.[1] In a majority of the cases, rigid organic linkers have been used to control the shape and symmetry of the final assemblies.[2] On the other hand, flexible linkers are less predictable in self-assembly and have a tendency to form undesired polymer. However, flexible linkers may generate pseudorigid assemblies[3] that can distort their shapes to obtain a more thermodynamically stable conformation for host−guest interactions. Moreover, properties of a molecule depend on the existing functional group(s). Thus, incorporation of functional groups in nanostructures may be an efficient way to guide the properties of the resulting assemblies. Several functional groups[4] like porphyrin, calixarene, and acid-based receptors have been incorporated into self-assemblies. Recently, we have introduced amide functionality into 3D Pd cages.[5] However, incorporation of ester functionality to nanostructures of Pd(II) and Pt(II) is rare except for a very few ester-based open frameworks reported recently.[6]

Here we report the design and synthesis of a new tripodal ester linker *N*,*N*′,*N*″-tris(4-pyridylmethyl) trimesic ester (**1a**) and its self-assembly with a C_4 symmetric naked Pd(II)-nitrate to a face-directed nanoscopic molecular ball (**2a**). To the best of our knowledge **2a** represents the first example of a 3D Pd(II) cage (close framework) containing ester functionality. An analogous cage (**2b**) was also prepared by using a tripodal amide linker *N*,*N*′,*N*″-tris(3-pyridylmethyl) trimesic amide (**1b**).

Results and Discussion

Edge-directed and face-directed self-assembly are the two distinct processes in the synthesis of supramolecular species. Using the former one, several 3D assemblies like molecular dodecahedron,[7] cube,[8] adamantanoid,[9a] double-square,[9b] and trigonal bipyramidal[5] cages have been synthesized. On the other

10.1021/jo061311g CCC: $33.50
Published on Web 10/06/2006

hand, face-directed assemblies are less common. In this paradigm, some or all the faces of the target assemble are spanned by the linkers themselves, which hold together the overall structure.[10] Our selection of the two tripodal linkers (**1a** and **1b**) is basically due to two reasons: the first is to introduce ester/amide functionality and flexibility into the 3D nanostructure and the second is to use a pseudoflat tritopic linker that can fit well on the eight trigonal faces of a ball.

To align eight tritopic donor linkers on the trigonal faces of a ball, we prepared ligands **1a**,**b** by the reaction of trimesyl chloride and an appropriate alcohol/amine using excess triethylamine (see Scheme 1).

When intense orange ligand **1a** (0.04 mmol) was treated with $Pd(NO_3)_2$ (0.03 mmol) in DMSO-d_6 (1.5 mL) for 2 h at 60 °C, the formation of a single product (Scheme 2) (very light yellow,

SCHEME 1. Synthesis of Tritopic Donor Linkers 1a and 1b

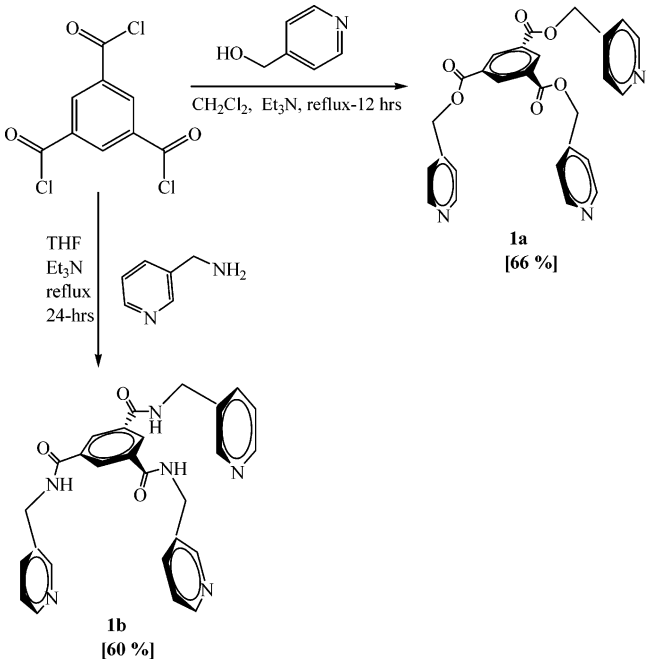

SCHEME 2. Self-Assembly of Nanoballs (2a and 2b)[a]

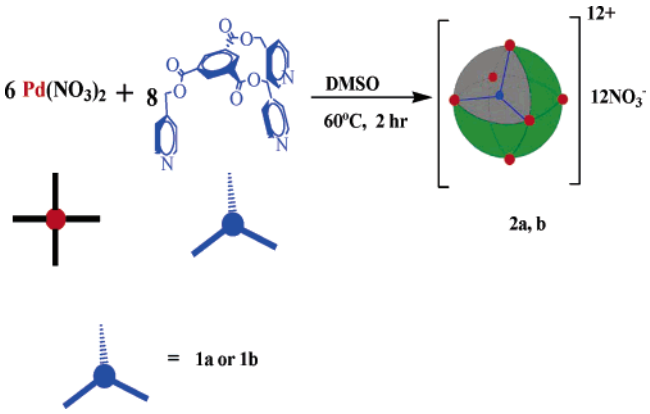

[a] Grey represents one of the eight trigonal faces each of which is occupied by a tritopic linker (blue).

2a) was indicated by ^{1}H NMR spectroscopic analysis (Figure 1). Similarly, reaction of $Pd(NO_3)_2$ with **1b** in a 3:4 molar ratio in DMSO-d_6 yielded **2b**, which was also characterized by NMR and IR spectroscopy.

The four proton signals (H_{a-d}) observed in **2a** (Figure 1) indicate that all the ligands are located in an identical fashion in the product and are in a symmetry environment identical with the parent ligand. The overall downfield shift ($\Delta\delta_{py\alpha} = 0.6$ and 0.7 ppm for **2a** and **2b** respectively) of the pyridinyl proton

(1) (a) Seidel, S. R.; Stang, P. J. *Acc. Chem. Res.* **2002**, *35*, 972. (b) Leininger, S.; Olenyuk, B.; Stang, P. J. *Chem. Rev.* **2000**, *100*, 853. (c) Stang, P. J.; Olenyuk, B. *Acc. Chem. Res.* **1997**, *30*, 502. (d) Swiegers, G. F.; Malefetse, T. J. *Coord. Chem. Rev.* **2002**, *225*, 91. (e) Cotton, F. A.; Lin, C.; Murillo, C. A. *Acc. Chem. Res.* **2001**, *34*, 759. (f) Badjic, J. D.; Nelson, A.; Cantrill, S. J.; Turnbull, W. B.; Stoddart, J. F. *Acc. Chem. Res.* **2005**, *38*, 723. (g) Cantrill, S. J.; Chichak, K. S.; Peters, A. J.; Stoddart, J. F. *Acc. Chem. Res.* **2005**, *38*, 1. (h) Fujita, M.; Umemoto, K.; Yoshizawa, M.; Fujita, N.; Kusukawa, T.; Biradha, K. *Chem. Commun*. **2001**, 509. (i) Uller, E.; Demleitner, I.; Bernt, I.; Saalfrank, R. W. Synergistic Effect of Serendipity and Rational Design in Supramolecular Chemistry. In *Structure and Bonding*; Fujita, M., Ed.; Springer: Berlin, Germany, 2000; Vol. 96, p 149. (j) Caulder, D. L.; Raymond, K. N. *J. Chem. Soc., Dalton Trans.* **1999**, 1185. (k) Caulder, D. L.; Raymond, K. N. *Acc. Chem. Res.* **1999**, *32*, 975. (l) Baxter, P. N. W.; Lehn, J.-M.; Baum, G.; Fenske, D. *Chem. Eur. J.* **1999**, *5*, 102. (m) Fujita, M. *Chem. Soc. Rev.* **1998**, *27*, 417. (n) Lehn, J.-M. *Supramolecular Chemistry*: *concepts and perspectives*; VCH: New York, 1995.

(2) (a) Mukherjee, P. S.; Das, N.; Kryschenko, Y. K.; Arif, A. M.; Stang, P. J. *J. Am. Chem. Soc.* **2004**, *126*, 2464. (b) Tominaga, M.; Suzuki, K.; Murase, T.; Fujita, M. *J. Am. Chem. Soc.* **2005**, *127*, 11950. (c) Chi, K. W.; Addicott, C.; Arif, A. M.; Das, N.; Stang, P. J. *J. Org. Chem.* **2003**, 68, 9798. (d) Tabellion, F. M.; Seidel, S. R.; Arif, A. M.; Stang, P. J. *J. Am. Chem. Soc.* **2001**, *123*, 7740. (e) Tabellion, F. M.; Seidel, S. R.; Arif, A. M.; Stang, P. J. *J. Am. Chem. Soc.* **2001**, *123*, 11982. (f) Hiraoka, S.; Fujita, M. *J. Am. Chem. Soc.* **1999**, *121*, 10239−10240. (g) Fujita, M.; Ibukuro, F.; Seki, H.; Kamo, O.; Imanari, M.; Ogura, K. *J. Am. Chem. Soc.* **1996**, *118*, 899. (h) Fujita, M.; Aoyagi, M.; Ibukuro, F.; Ogura, K.; Yamaguchi, K. *J. Am. Chem. Soc.* **1998**, *120*, 611. (i) Fujita, M.; Nagao, S.; Ogura, K. *J. Am. Chem. Soc.* **1995**, *117*, 1649. (j) Fujita, M.; Kwon, Y. J.; Sasaki, O.; Yamaguchi, K.; Ogura, K. *J. Am. Chem. Soc.* **1995**, *117*, 7287. (k) Bowyer, P. K.; Cook, V. C.; Naseri, N. G.; Gugger, P. A.; Rae, D. A.; Swiegers, G. F.; Willis, A. C.; Zank, J.; Wild, S. B. *Proc. Natl. Acad. Sci.* **2002**, *99*, 4877. (l) Das, N.; Mukherjee, P. S.; Arif, A. M.; Stang, P. J. *J. Am. Chem. Soc.* **2003**, *125*, 13950. (m) Bourgeois, J-P.; Fujita, M.; Kawano, M.; Sakamoto, S.; Yamaguchi, M. *J. Am. Chem. Soc.* **2003**, *125*, 9260.

(3) (a) Hiraoka, S.; Kubota, Y.; Fujita, M. *Chem. Commun*. **2000**, 1509. (b) Chand, D. K.; Fujita, M.; Biradha, K.; Sakamoto, S.; Yamaguchi, K. *Dalton Trans*. **2003**, 2750 and references therein. (c) Liu, H. K.; Tong, K. *Chem. Commun*. **2002**, 1316.

(4) (a) Fan, J.; Whiteford, J. A.; Olenyuk, B.; Levin, M. D.; Stang, P. J. *J. Am. Chem. Soc.* **1999**, *121*, 2741. (b) Stang, P. J.; Fan, J.; Olenyuk, B. *J. Chem. Soc., Chem. Commun*. **1997**, 1453. (c) Drain, C. M.; Lehn, J. M. *J. Chem. Soc., Chem. Commun*. **1994**, 2313. (d) Ikeda, A.; Udzu, H.; Zhong, Z.; Shinkai, S.; Sakamoto, S.; Yamaguchi, K. *J. Am. Chem. Soc.* **2001**, *123*, 3872. (e) Ikeda, A.; Yoshimara, M.; Tani, F.; Naruta, Y.; Shinkai, S. *Chem. Lett.* **1998**, 587. (f) Ikeda, A.; Yoshimara, M.; Udzu, H.; Fukuhara, C.; Shinkai, S. *J. Am. Chem. Soc.* **1999**, *121*, 4296. (g) Whiteford, J. A.; Stang, P. J.; Huang, S. D. *Inorg. Chem*. **1998**, *37*, 5595. (h) Schnebeck, R. D.; Randaccio, L.; Zangrando, E.; Lippert, P. *Angew. Chem., Int. Ed.* **1998**, *37*, 119. (i) Moon, D.; Kang, S.; Park, J.; Lee, K.; John, R. P.; Won, H.; Seong, G. H.; Kim, Y. S.; Kim, G. H.; Rhee, H.; Lah, M. S. *J. Am. Chem. Soc.* **2006**, *128*, 3530.

(5) Mukherjee, P. S.; Das, N.; Stang, P. J. *J. Org. Chem*. **2004**, *69*, 3526 and references therein.

(6) (a) Chatterjee, B.; Noveron, J. C.; Resendiz, M. J. E.; Liu, J.; Yamamoto, T.; Parker, D.; Cinke, M.; Nguyen, C. V.; Arif, A. M.; Stang, P. J. *J. Am. Chem. Soc.* **2004**, *126*, 10645. (b) Tashiro, S.; Tominaga, M.; Kusukawa, T.; Kawano, M.; Sakamoto, S.; Yamaguchi, M.; Fujita, M. *Angew. Chem., Int. Ed.* **2003**, *42*, 3267.

(7) (a) Olenyuk, B.; Levin, M. D.; Whiteford, J. A.; Shield, J. E.; Stang, P. J. *J. Am. Chem. Soc.* **1999**, *121*, 10434. (b) Two drops of the suspended solution (made by ultrasound) of the appropriate cage was put on a Cu grid and it was heated to evaporate the solvent and finally put under a microscope.

(8) (a) Eaton, P. E.; Cole, F. W. *J. Am. Chem. Soc.* **1964**, *86*, 3157. (b) Fleischer, E. B. *J. Am. Chem. Soc.* **1964**, *86*, 3889.

(9) (a) Schweiger, M.; Seidel, S. R.; Schmitz, M.; Stang, P. J. *Org. Lett.* **2000**, *2*, 1255. (b) Fujita, M.; Yu, S. Y.; Kusukawa, T.; Funaki, H.; Ogura, K.; Yamaguchi, K. *Angew. Chem., Int. Ed.* **1998**, *37*, 2082.

(10) Johannessen, S. C.; Brisbois, R. G.; Fischer, J. P.; Grieco, P. A.; Counterman, A. E.; Clemmer, D. E. *J. Am. Chem. Soc.* **2001**, *123*, 3818.

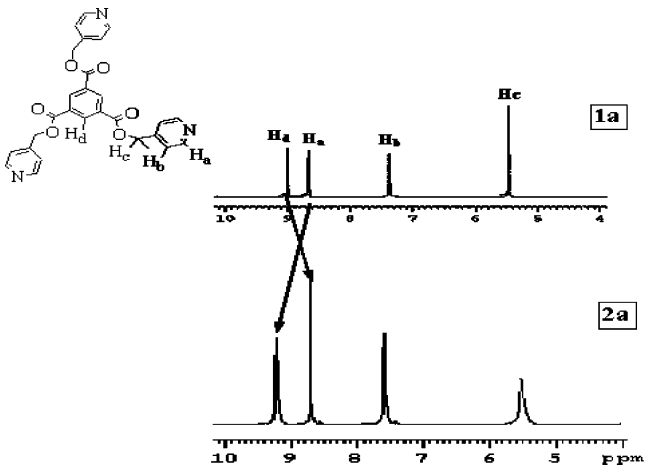

FIGURE 1. ^{1}H NMR of **1a** (top) and **2a** (bottom).

signals in both cases indicated the coordination of the ligand to metal ions. Hetero-COSEY revealed the diastereotopic nature of the H_c protons of **2b** (Supporting Information). Moreover, in the IR spectrum of the cages the absorption arising from the ester/amide group was observed. The C═O stretching frequency of **1a** appeared at 1706 cm^{-1}, whereas the corresponding stretching frequency in **2a** was found at 1731 cm^{-1}. Similarly, the C═O stretching frequency in **2b** is 1658 cm^{-1}, which is 30 cm^{-1} more than the parent amide **1b**. This shift of the C═O stretching to higher frequency is consistent with the withdrawal of electron density from the pyridine nitrogen by the Pd metal center via the N−Pd dative bond formation. In case of **2b**, broadening of the proton peaks was probably due to inter-/intramolecular hydrogen bonding.

While NMR spectroscopy provides a first insight about the metal−ligand coordination and formation of a single product, it does not provide any information about the shape of this kind of product. ESI mass spectrometry has proven to be a useful tool in the corroboration of structural assignments for this kind of self-assemblies.[11] Electrospray mass spectroscopy clearly confirmed a $Pd_6(\mathbf{1})_8(NO_3)_{12}$ composition with the molecular mass of 5250.36 and 5226.36 Da for **2a** and **2b**, respectively. The ESI-mass spectra of **2a** and **2b** (Figure 1) showed signals corresponding to the consecutive loss of nitrate counterions, $[M - 3NO_3]^{3+}$, $[M - 4NO_3]^{4+}$, $[M - 5NO_3]^{5+}$, and $[M - 6NO_3]^{6+}$; for **2a**, $[M - 3NO_3]^{3+}$ [*m/z* 1687.42 (calcd 1688.12)], $[M - 4NO_3]^{4+}$ [*m/z* 1250.25 (calcd 1250.59)], $[M - 5NO_3]^{5+}$ [*m/z* 987.75 (calcd 988.07)], $[M - 6NO_3]^{6+}$ [*m/z* 812.75 (calcd 813.02)]; and for **2b**, $[M - 3NO_3]^{3+}$ [*m/z* 1680.33 (calcd 1680.12)], $[M - 4NO_3]^{4+}$ [*m/z* 1244.33 (calcd 1244.59)], $[M - 5NO_3]^{5+}$ [*m/z* 983.17 (calcd 983.27)], $[M - 6NO_3]^{6+}$ [*m/z* 809.00 (calcd 809.06)]. Our attempt to prepare a similar cage using rigid tripodal linker tris(4-pyridyl)methanol in combination with Pd(II) was unsuccessful; only an insoluble polymeric product was obtained. So, both the flat (aromatic) part of the tritopic linker as well as the flexible ester/amide functionalities are important factors for the formation of this kind of ball. The former is required to fit on the trigonal faces of a ball and the flexibility helps to maintain the C_4 symmetry of the square-planar Pd(II) center.

Several attempts to grow suitable single crystals for X-ray diffraction failed and only in the case of **2a** microcrystalline was product obtained. MM2 force field simulations[9] were employed to visualize the size and shapes of the cages. The $Pd_6(\mathbf{1a})_8(NO_3)_{12}$ composition of **2a** yielded the shape of a nanoscopic ball (Figure 3) with six C_4 symmetric centers each occupied by a Pd(II) ion and eight C_3 symmetric trigonal faces occupied by **1a**. A similar shape was also obtained for **2b** (see Supporting Information) by energy-minimized MM2 calculations. The predicted diameter of **2a** is 2.1 nm and the volume of the sphere is approximately 4851 Å^3 while for **2b** the diameter is 1.8 nm. The opposite Pd−Pd distance measured the diameter.

Transmission electron microscopy (TEM) has become a useful technique in providing valuable information on the size and shape of nanoensembles.[7] A clear TEM[7b] image of **2a** was observed (Figure 4), strongly supporting the formation of a 2−2.5 nm molecular particle, which was also implied by MM2 force field calculation. TEM image of **2b** also suggested the formation of a spherical molecule of around 2 nm (Supporting Information). Elemental analyses reveled the presence of 12 solvated DMSO molecules in **2a** whereas no solvent was found in **2b**. TGA also confirmed the presence of 12 DMSO molecules by the appropriate amount of weight loss between 190 and 260 °C. This weight loss was due to the removal of DMSO and was also confirmed by mass analysis of the evolved molecule by a mass spectrometer directly attached to the TG instrument. The reversible solvation (DMSO) was found for the desolvated **2a**.[12] The cage is stable up to 270 °C (see the Supporting Information). Upon formation, molecular cage **2a** assumes a less intense yellow color. The absorption spectrum of **2a** showed (see the Supporting Information) a significant decrease in absorbance relative to **1a** after complex formation. The absorbance in the electronic spectrum exhibited a near-UV transition, which is red-shifted relative to **1a**. Host−guest experiments revealed that **2** (both **2a** and **2b**) could efficiently interact with a cationic guest, NEt_4^+ (**3**), despite their positive charge. Treatment of excess (5 equiv) NEt_4NO_3 with a DMSO solution of **2** resulted in the quantitative accommodation of one **3** per molecule of cage **2**. The inclusion complexes $(\mathbf{2}\cdot\mathbf{3})^{13+}$ were identified by ^{1}H NMR spectroscopy, which showed a new downfield shifted set of signals for **3** with a 1:1 host−guest ratio (see the Supporting Information). This downfield shift of proton signals is due to the interaction of the protons of **3** with the ester/amide moieties of the cages **2**. However, no clear NOESY correlation between the protons of **3** and phenyl rings of the cages **2** was found. The inclusion complex was isolated in a pure form by acetone addition and characterized.

In conclusion, we report the first flexible, Pd(II)-based close framework cage incorporating ester functionality using a new tripodal ester **1a**. An analogous nanoball using *N*′,*N*′,*N*′′-tris-(3-pyridylmethyl) trimesic amide linker was also prepared. NMR, ESI-mass spectrometry, TEM, and MM2 force field calculations support the formation of nanoballs with eight trigonal faces occupied by C_3 symmetric donor linkers. Despite their tendency to form polymers, ligands **1a** and **1b** self-assemble into cages. The use of flexible ester and amide linkers with Pd(II)/Pt(II) metals and the formation of nanocages has the potential to expand the coordination driven self-assembly

(11) (a) Jude, H.; Disteldorf, H.; Fischer, S.; Wedge, T.; Hawkridge, A. M.; Arif, A. M.; Hawthorne, M. F.; Muddiman, D. C.; Stang, P. J. *J. Am. Chem. Soc.* **2005**, *127*, 12131. (b) Jude, H.; Sinclair, D. J.; Das, N.; Sherburn, M. S.; Stang, P. J. *J. Org. Chem.* **2006**, *71*, 4155.

(12) The desolvated **2b** was soaked in DMSO for 30 min and then washed several times with acetone and dried completely. TGA and elemental analyses of the dry product showed the reversible solvation by DMSO.

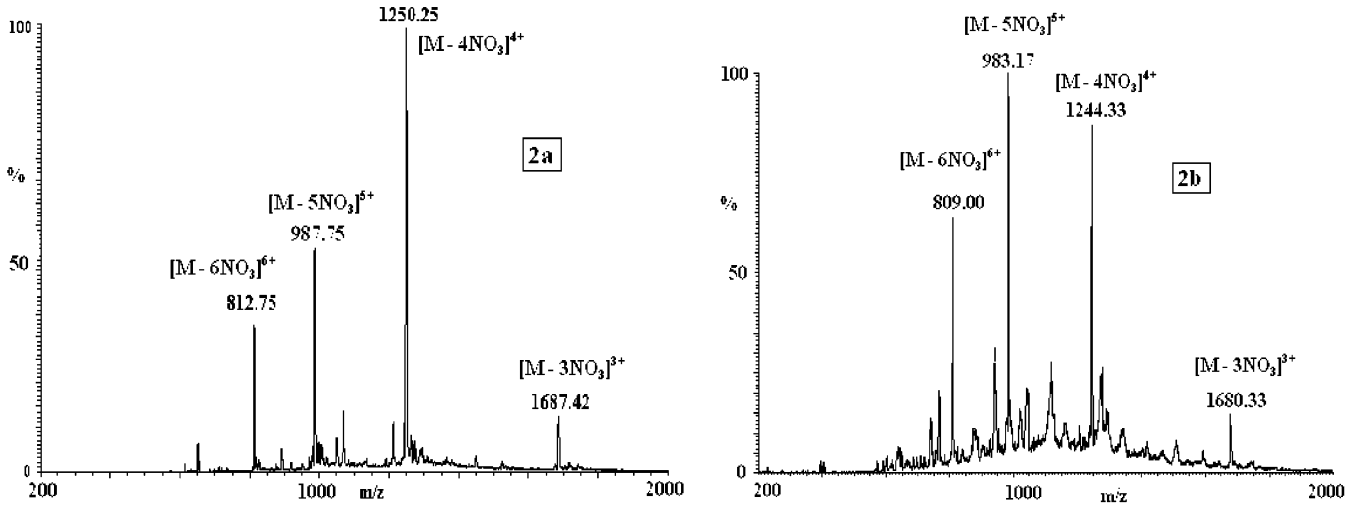

FIGURE 2. ESI-mass spectra of the assemblies **2a** (left) and **2b** (right).

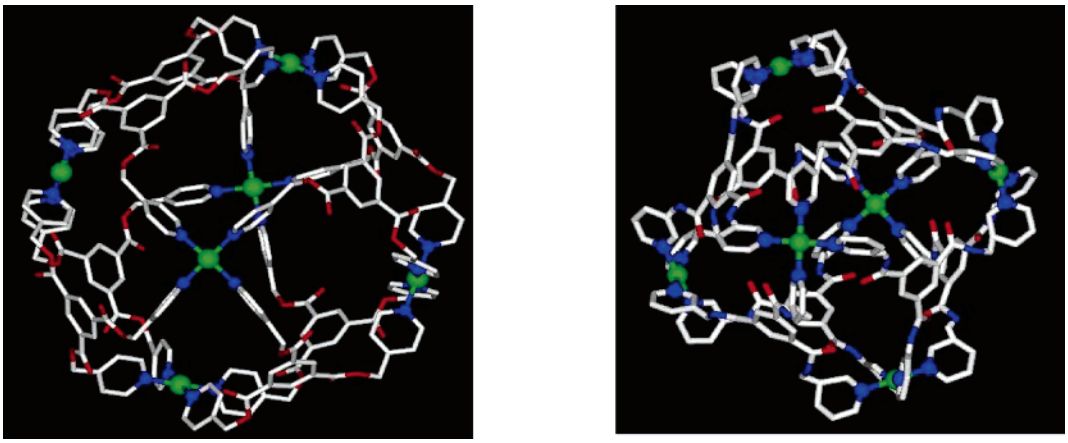

FIGURE 3. Molecular view of the nanoballs **2a** (left) and **2b** (right) (green = Pd, red = O, blue = N, white = C).

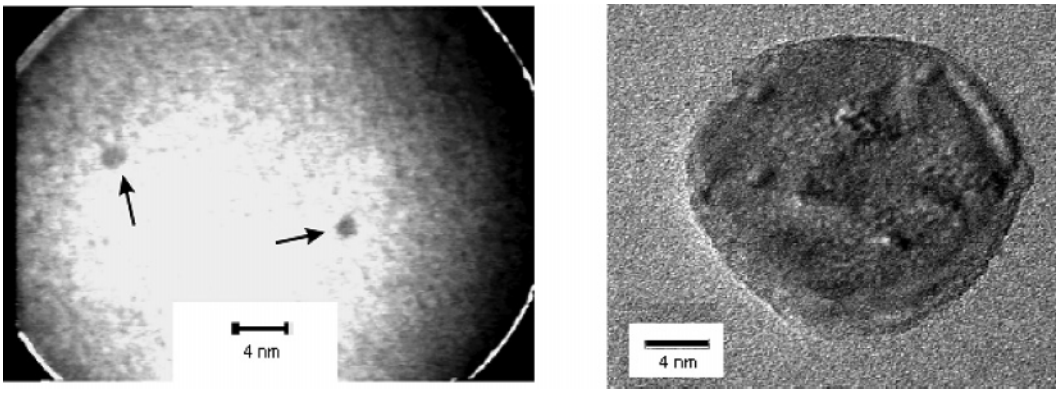

FIGURE 4. Transmission electron microscopic view of **2a** (left) and **2b** (right).

for the construction of novel materials for practical application like gas adsorption, catalysis, and host−guest chemistry.

Experimental Section

Synthesis of 1a. To a stirred solution of trimesyl chloride (0.66 g, 2.50 mmol) in dry dichloromethane (50 mL) was added triethylamine (1.12 mL, 8 mmol) under nitrogen atmosphere followed by the addition of 4-pyridylcarbinol (7.5 mmol, 0.82 g). This mixture was then stirred under nitrogen for 1 h and then refluxed for 12 h under nitrogen. The solution was washed with water and extracted twice with saturated $KHCO_3$ solution. The organic part was dried over anhydrous K_2CO_3 and filtered. The solvent was removed and the product was crystallized from a methanol/dichloromethane mixture. Yield: 66%. Anal. Calcd for $C_{27}H_{21}O_6N_3$: C, 67.08; H, 4.3; N, 8.6. Found: C, 67.33; H, 4.42; N, 8.35. ^{1}H NMR (DMSO-d_6): δ 8.99 (s, 3H), 8.66 (d, 6H), 7.37 (d, 6H), 5.46 (s, 6H). ^{13}C NMR (DMSO-d_6): δ 163.0, 149.8, 143.2, 135.0, 130.0, 121.1, 63.1 ppm. IR (KBr): ν(C=O), 1706 cm^{-1}. ESI: 484.2 [M + H$^+$].

Synthesis of 1b. To a stirred solution of trimesyl chloride (0.90 g, 3.39 mmol) in dry THF (50 mL) was added triethylamine (1.6 mL, 11.2 mmol) and then 3-aminomethylpyridine (1.09 g, 10.2 mmol) was added under nitrogen atmosphere. This mixture was stirred for 1 h at room temperature and then refluxed for 24 h. The white precipitate was filtered and washed several times with water to remove the byproduct Et_3NHCl. Then the white solid was dried under vacuum. Yield: 60%. Anal. Calcd for $C_{27}H_{24}O_3N_6$: C, 67.50; H, 4.00; N, 17.5. Found: C, 67.34; H, 4.86; N, 17.4. ^{1}H NMR (DMSO-d_6): δ 9.5 (s, 3H), 8.70 (d, 3H), 8.60 (s, 3H), 8.56 (d, 3H), 7.80 (m, 3H), 7.50 (d, 3H), 4.60 (s, 6H). ^{13}C NMR (DMSO-d_6): δ 166.3, 147.3, 146.7, 135.5, 134.2, 128.1, 123.1, 121.0, 40.0 ppm. IR (KBr): ν(C═O), 1628 cm^{-1}; ν(NH), 3061 cm^{-1}. ESI: 481.0 [M + H$^+$].

General Procedure for the Preparation of Cage 2a and 2b. To a 2 mL DMSO solution containing 7.98 mg (0.03 mmol) of $Pd(NO_3)_2$ was added a DMSO solution (1 mL) of either **1a** or **1b** (0.04 mmol) drop-by-drop with continuous stirring. The mixture was stirred for 2 h and adding acetone precipitated the product.

2a: Yield: (26.4 mg) 97%. Anal. Calcd for $Pd_6C_{240}H_{240}N_{36}O_{96}S_{12}$: C, 46.54; H, 3.8; N, 8.14; S, 6.2. Found: C, 46.32; H, 3.92; N, 8.23; S, 6.38. ^{1}H NMR (DMSO-d_6): δ 9.26 (d, 6H), 8.70 (s, 3H), 7.60 (d, 6H), 5.55(s, 6H). ^{13}C NMR (DMSO-d_6): δ 163.1, 151.9, 150.0, 134.0, 130.0, 122.0, 63.1 ppm. IR (KBr): ν-(C═O), 1731 cm^{-1}.

2b: Yield: (26.0 mg) 96%. Anal. Calcd for $Pd_6C_{216}H_{192}N_{60}O_{60}$: C, 49.59; H 3.67; N, 16.07. Found C, 49.43; H, 3.62; N, 16.23. ^{1}H NMR (DMSO-d_6): δ 9.9 (br, 3H), δ 9.6 (br, 3H), 9.3 (br, 3H), 8.4(br, 3H), 8.1 (br, 3H), 7.7 (br, 3H), 4.6 (br, 6H) ppm. ^{13}C NMR (DMSO-d_6): δ 166.0, 151.0, 150.2, 139.9, 139.0, 134.7, 129.4, 126.8, 40.0 ppm. IR (KBr): ν(C═O), 1658 cm^{-1}; ν(NH) 3042 cm^{-1}.

Acknowledgment. Financial support from the DST, Government of India, and the Indian Institute of Science, Bangalore is gratefully acknowledged. We thank Mr. B. R. Mohan of Thermo Electron Corporation, Bangalore Division, for assistance with the electrospray mass spectra.

Supporting Information Available: General experimental method, ^{1}H NMR (for **1b** and **2b**), and ^{13}C NMR for **1a**, **1b**, **2a**, and **2b** (five figures); TGA and UV−vis spectra for **2a**. This material is available free of charge via the Internet at http://pubs.acs.org.

JO061311G